02

$YAl_3(BO_3)_4$: Cr crystals for luminescent cryothermometry

© A.D. Molchanova[1], M. Diab[1,2], K.N. Boldyrev[1], M.N. Popova[1]

[1] Institute of Spectroscopy, Russian Academy of Sciences,
Troitsk, Moscow, Russia
[2] Moscow Institute of Physics and Technology (National Research University),
Dolgoprudny, Moscow Region, Russia

e-mail: nastyamolchanova@list.ru

Received April 19, 2024
Revised April 26, 2024
Accepted April 27, 2024

The luminescence spectra of the $YAl_3(BO_3)_4 : Cr^{3+}$ crystal have been registered in the spectral range of $^2E \rightarrow {}^4A_2$ electronic transitions in Cr^{3+} ions ($14550-14700\,cm^{-1}$) with high spectral resolution at temperatures 4–300 K. The temperature dependences of the ratios of the integral intensities of lines R_2 and R_1, as well as N' and N (presumably the lines of the $^2E \rightarrow {}^4A_2$ transitions of the Cr^{3+} center in a position distorted due to the vicinity of a some defect), correspond well to the Boltzmann distribution. On the measurement of these ratios, a ratiometric thermometer with a maximum absolute sensitivity at temperatures 40.3 and 21.6 K, respectively, and a relative sensitivity of up to $12\%\,K^{-1}$ can be realized. Measuring the width of the most intense spectral component — line R_1 — can be a way to capture temperature in the range of 100 K and above.

Keywords: luminescent cryothermometry, $YAl_3(BO_3)_4 : Cr^{3+}$ crystal, high-resolution Fourier-transform spectroscopy.

DOI: 10.61011/EOS.2024.04.58881.6314-24

Introduction

While a wide variety of compounds doped with *d* ions are available, the majority of studies in the field of luminescent thermometry performed to date have been focused on compounds with Cr^{3+} ions. This is attributable to the excellent light-emitting ability of Cr^{3+} ions, their wide absorption spectrum, and high sensitivity of the luminescence spectrum to temperature. In most cases, thermometry based on compounds with Cr^{3+} ions is carried out within the temperature range relevant for biological applications ($> 0^\circ C$) by measuring the intensity ratio of the $^2E \rightarrow {}^4A_2$ and $^4T_2 \rightarrow {}^4A_2$ transition bands [1–8]. Crystals doped simultaneously with Cr^{3+} ions and various rare-earth ions, such as Eu^{3+} [9,10] and Yb^{3+} [11], were proposed for thermometry in a number of studies. The temperature was determined by measuring the ratio of luminescence intensities of chromium ions and rare-earth ions. Only a few studies focused on the construction of ratiometric luminescent thermometers based on the intensity ratio of R_1 and R_2 lines (transitions from split orbital doublet ^2E to ground singlet $^4A_2$) have been published [4,12–15]. The majority of experiments were performed at temperatures above 80 K. Low-temperature (down to 4 K) thermometry was examined for Al_2O_3, Ga_2O_3, $Y_3Al_5O_{12}$, and $YAlO_3$ compounds doped with chromium [13]. Temperature was determined in three ways: by the shift of the R_1 line, by the ratio of intensities of lines R_1 and R_2, and by the decay time of these lines. Low-temperature thermographic studies of Al_2O_3:Cr coatings obtained by plasma electrolytic oxidation have also been performed [12]. $YAl_3(BO_3)_4$:Cr^{3+} (YAB:Cr^{3+}) crystals have been used in experiments combining luminescent thermometry with optical heating. Temperature was determined by measuring the ratio of intensities of bands $^2E \rightarrow {}^4A_2$ and $^4T_2 \rightarrow {}^4A_2$ within the $-150-300^\circ C$ range [1]. No studies into the thermometric properties of YAB:Cr^{3+} at cryogenic temperatures involving the measurement of parameters of fine structure components of the $^2E \rightarrow {}^4A_2$ transition in an Cr^{3+} ion have been carried out yet.

The Boltzmann ratiometric thermometry method was proven to be the best suited for non-contact measurements of low temperatures [16]. Temperature dependences of the ratio of equilibrium populations $n_2(T)/n_1(T)$ and, consequently, the luminescence intensity ratio (LIR) for two chosen levels with energies E_2 and E_1 in this case follow the Boltzmann distribution:

$$LIR(T) = \frac{I_2(T)}{I_1(T)} = \frac{W_2 n_2(T)}{W_1 n_1(T)} = Ce^{(-\Delta E/kT)}, \qquad (1)$$

where $C = W_2/W_1$ is the temperature-independent ratio of transition probabilities, $\Delta E = E_2 - E_1$, and k is the Boltzmann constant.

The absolute thermal sensitivity is then defined as

$$S_a(T) = \frac{dLIR(T)}{dT} = \frac{\Delta E}{kT^2} LIR(T) \qquad (2)$$

and reaches its maximum at temperature $T_m = \Delta E/2k$. Thermometers utilizing different measurement principles are compared in terms of relative thermal sensitivity

$$S_r(T) = \frac{1}{LIR} \times \frac{dLIR(T)}{dT} = \frac{\Delta E}{kT^2}. \qquad (3)$$

In the present study, the application of fine structure components of luminescence spectra of yttrium aluminum borate YAB:Cr^{3+} crystals in the region of $^2E \rightarrow {}^4A_2$ transitions in Cr^{3+} ions as levels E_1 and E_2 is considered. In addition, the feasibility of temperature measurement based on the width of the most intense spectral component (R_1) is discussed.

Experimental procedure

Crystals of $YAl_3(BO_3)_4$:Cr were grown by the solution-melt method in the laboratory of L.N. Bezmaternykh at the Kirensky Institute of Physics (Siberian Branch, Russian Academy of Sciences) in Krasnoyarsk. They were not doped deliberately with chromium. The inclusion of Cr^{3+} ions in the YAB structure is attributable to their presence in the composition of the Al_2O_3 reagent (the concentration indicated in the certificate is 0.001%). Luminescence spectra were recorded with a spectral resolution of 0.1 cm^{-1} using a Bruker IFS 125 HR Fourier spectrometer within the spectral range of the $^2E \rightarrow {}^4A_2$ transition in Cr^{3+} ions (14550–14700 cm^{-1}). A CaF_2 beam splitter and a high-gain InGaAs detector were used to record the spectra. The sample was cooled in a Sumitomo SRP096 closed helium cycle cryostat to a temperature of 4 K.

Luminescence spectra were recorded in the temperature ranges of 4 K → 10 K, 10 K → 40 K, 40 K → 70 K, and 70 K → 300 K; the temperature step was 0.5, 2, 4, and 10 K, respectively. To reduce the thermal load on the sample, a double polished cold screen with small apertures for radiation input and output was installed. The sample was glued with silver paste to the copper finger of the cryostat. Temperature was measured using a calibrated LakeShore DT-670 diode temperature sensor, which was mounted in close proximity to the sample, and controlled and recorded by a LakeShore 335 PID temperature controller. The accuracy of temperature control was ±0.05 K. Luminescence was excited by a diode laser with a power of 75 mW, a wavelength of 450 nm, and a spectrum width of 15 nm; the focal spot had a diameter of 1 mm.

Results and discussion

Yttrium aluminum borate $YAl_3(BO_3)_4$ crystals have the structure of the huntite mineral ($CaMg_3(CO_3)_4$) with non-centrosymmetric space group $R32$ of the trigonal system [17]. Figure 1 shows the unit cell of the YAB crystal. The crystal structure is formed by layers perpendicular to crystallographic axis c and consisting of distorted YO_6 prisms, AlO_6 octahedra, and two types of BO_3 groups ($B1O_3$ and $B2O_3$). Y^{3+} ions in YO_6 prisms are surrounded by six oxygen ions of the same type and occupy sites with point symmetry group D_3 (Figs. 1, *b, c*). The point group of the site of Al^{3+} ions in AlO_6 – C_2 (Figs. 1, *b, c*). AlO_6

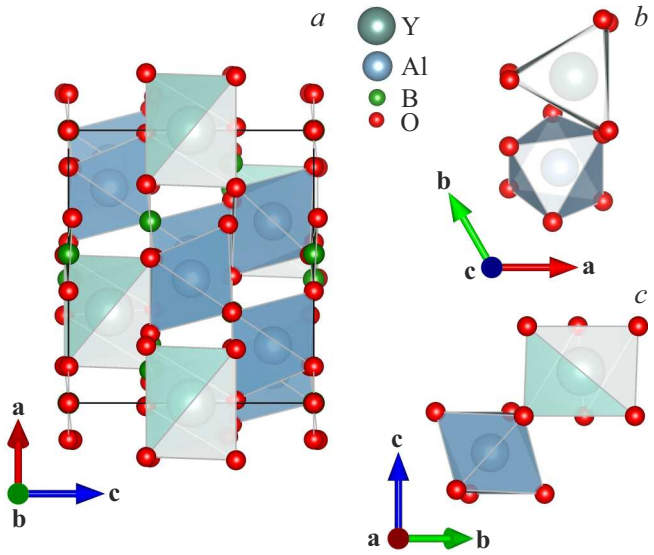

Figure 1. Projections of the unit cell of $YAl_3(BO_3)_4$ along axis b (a). Projections of the YO_6 trigonal prism and the AlO_6 distorted octahedron in the unit cell of $YAl_3(BO_3)_4$ along axes c (b) and a (c).

octahedra with common edges form spiral chains extending along axis c. Y^{3+} ions are located between three such chains and link them together. YO_6 prisms are isolated and have no common oxygen atoms. It was assumed in published studies on YAB:Cr spectroscopy that Cr^{3+} ions occupy Al^{3+} sites. Al^{3+} and Cr^{3+} ions have similar ionic radii (0.54 and 0.62 Å respectively), while the ionic radius of Y^{3+} is 0.9 Å [18]. The results of electron paramagnetic resonance (EPR) experiments also revealed that Cr^{3+} ions occupy octahedral sites in the YAB [19] structure; i.e., they substitute for Al^{3+} ions.

Descriptions of spectra in the region of R lines of a Cr^{3+} ion in YAB:Cr have already been presented in [20–22], but a detailed study of the temperature dependence of the structure of these spectra has not been performed. These data are needed to gain an insight into the feasibility of construction of ratiometric thermometers based on measuring the parameters of R lines.

A number of narrow lines and an adjacent broad band are seen in the red region of the YAB:Cr luminescence spectrum at low temperatures. This spectrum is associated with zero-phonon lines of transitions from excited orbital doublet ^2E to ground singlet $^4A_2$ of Cr^{3+} ions and the corresponding vibronic wings. In the present study, we analyze the zero-phonon lines of transition $^2E \rightarrow {}^4A_2$. A more detailed view of the spectrum (including the vibronic band) was presented, e.g., in our recent study [23] focused on the spectroscopic examination of a YAB:Mn crystal with an uncontrolled impurity (Cr^{3+} ions). The luminescence spectrum of the YAB:Cr crystal studied here has the same shape in the range of zero-phonon and vibronic $^2E \rightarrow {}^4A_2$ transitions. Figure 2 presents the luminescence spectra of YAB:Cr within the 14500–14700 cm^{-1} spectral range. The

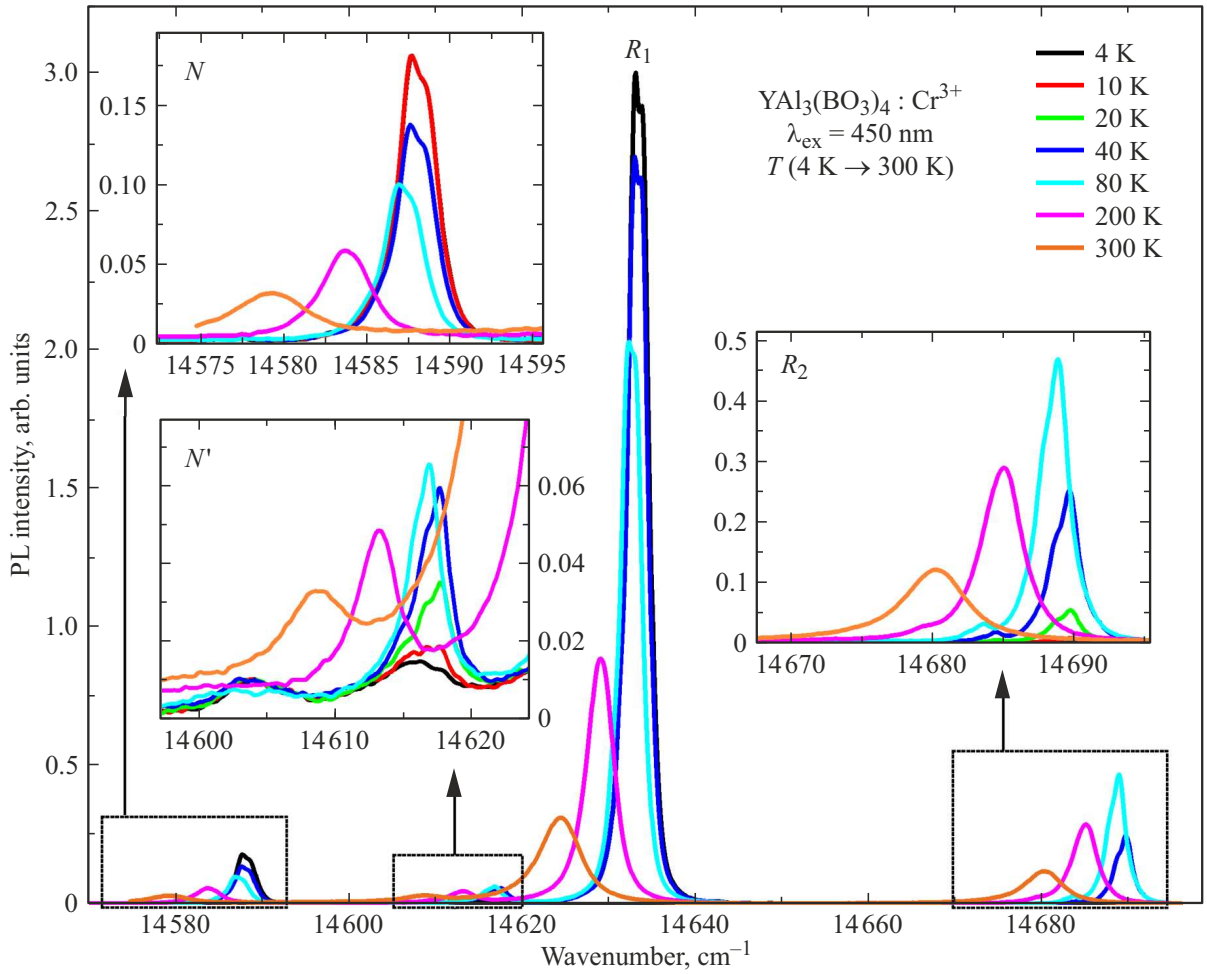

Figure 2. Photoluminescence spectra of a YAB:Cr crystal within the 14550–14700 cm^{-1} frequency range at temperatures of 4, 10, 20, 40, 80, 200, and 300 K. The excitation wavelength is λ_{ex} = 450 nm. Weak lines are shown in an enlarged scale in the insets.

splitting of doublet ^2E by low-symmetry components of the crystal field leads to the emergence of lines designated in literature as R_1 and R_2. The recorded positions of these lines at 4 K are 14633 and 14689 cm^{-1}, respectively. This is consistent with the positions of the R_1 and R_2 lines determined elsewhere [20–22]. In the low-frequency part of the spectrum, one can see the N line with a maximum frequency of 14588 cm^{-1} at 4 K. Such lines have been observed previously in several other chromium-doped crystals and identified as the lines of paired Cr^{3+} centers (N lines) [24–26] or single Cr^{3+} centers at sites distorted under the influence of a nearby crystal lattice defect [27]. In addition, a weak N' line with a maximum frequency of 14618 cm^{-1} at 4 K is seen on the low-frequency side of the R_1 line. Spectral bands R_1, R_2, N, and N' have a complex shape. Their decomposition into components is shown in Fig. 3. It is evident that these bands consist of two overlapping lines with a frequency interval of about 1 cm^{-1} between them. According to the results of EPR studies, the splitting of the Cr^{3+} ground state in YAB is 1.05±0.04 cm^{-1} at room temperature [19]. Owing to a strong exchange interaction, significantly greater magnitudes of splitting of the ground state are typical of paired centers of Cr^{3+} ions. For example, the magnitude of such splitting for different paired centers of chromium ions in ruby varies from 43 to 69 cm^{-1} [28].

Thus, lines N and N' apparently correspond not to paired Cr^{3+} centers, but to single Cr^{3+} centers at sites distorted by a certain proximate defect, and the observed doublets are associated with spin-orbit splitting of the $^4A_2$ ground state to which transitions from states ^2E are realized.

Figure 4 illustrates the temperature dynamics of YAB:Cr luminescence spectra in the region of R lines of Cr^{3+}. All lines shift to higher frequencies and narrow down as the temperature decreases. The width and position of lines remain virtually unchanged below 75 K. Line R_1, which is the most intense one in the spectrum, loses in intensity as the temperature grows from 4 K to room levels. This is attributable to the thermal redistribution of populations of components of the ^2E split level. Notably, the R_2 line intensity increases upon heating up to 75 K and decreases at higher temperatures. Apparently, this indicates a reduction

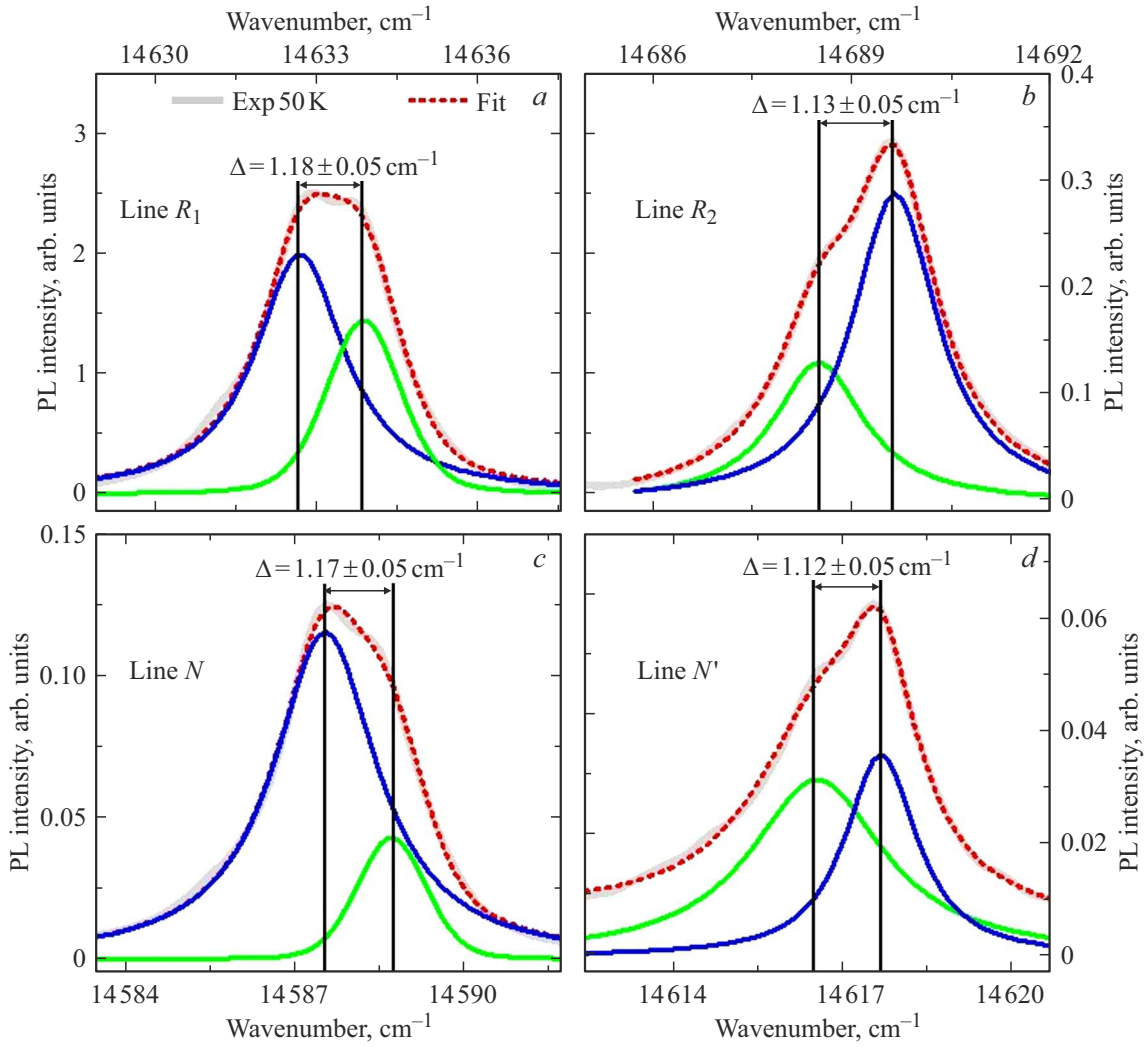

Figure 3. Structure of luminescence lines of a Cr^{3+} ion in YAB:Cr: R_1 (a), R_2 (b), N (c), and N' (d). Experimental spectra (red curves) are presented as the sum (dashes) of two profiles.

in the population of the upper ^2E component due to the redistribution of populations of ^2E levels in favor of vibronic ones. The temperature dynamics of lines N and N' is the same as the one of lines R_1 and R_2, respectively.

Luminescence lines R_1 and R_2 originate at levels separated by energy interval $\Delta E = 56\,\text{cm}^{-1}$. Figure 5, a presents the temperature dependence of ratio $LIR(T)$ of integral intensities of lines R_2 and R_1. It is evident that this dependence corresponds to the Boltzmann distribution for the $\Delta E = 56\,\text{cm}^{-1}$ interval. The temperature dependences of absolute and relative sensitivities are shown in Fig. 5, b. The maximum absolute sensitivity is achieved at $T_\text{m} = \Delta E/2k = 40.3\,\text{K}$, while relative sensitivity $S_\text{r}(T_\text{m})$ is 5% K^{-1} at this temperature. Thus, a thermometer measuring the ratio of integral intensities of the R_2 and R_1 lines will be the most efficient at low temperatures around 40 K.

Higher temperatures may be determined by measuring the width of the R_1 line. The width of all lines remains virtually unchanged within the 4–75 K temperature range and starts increasing noticeably at higher temperatures due to the enhancement of contribution of phonon processes. Let us examine the most intense line in the spectrum. Figure 6, a shows the temperature dependence of the half-width (full width at half maximum) of the R_1 line. The width remains virtually unchanged at 2.3 cm^{-1} within the 4–75 K temperature range. This translates into an almost zero absolute sensitivity at these temperatures (Fig. 6, b). Within the 75–300 K temperature range, the width increases smoothly from 2.3 to 32 cm^{-1}. The maximum relative sensitivity does not reach its maximum within the examined temperature range and assumes a value of 2% K^{-1} at 300 K.

The measurement range may be expanded to lower temperatures by probing the relative intensity of luminescence lines N' and N, which are separated by spectral interval $\Delta E = 30\,\text{cm}^{-1}$. Figure 7, a presents the temperature dependence of ratio $LIR(T)$ of integral intensities of lines N'

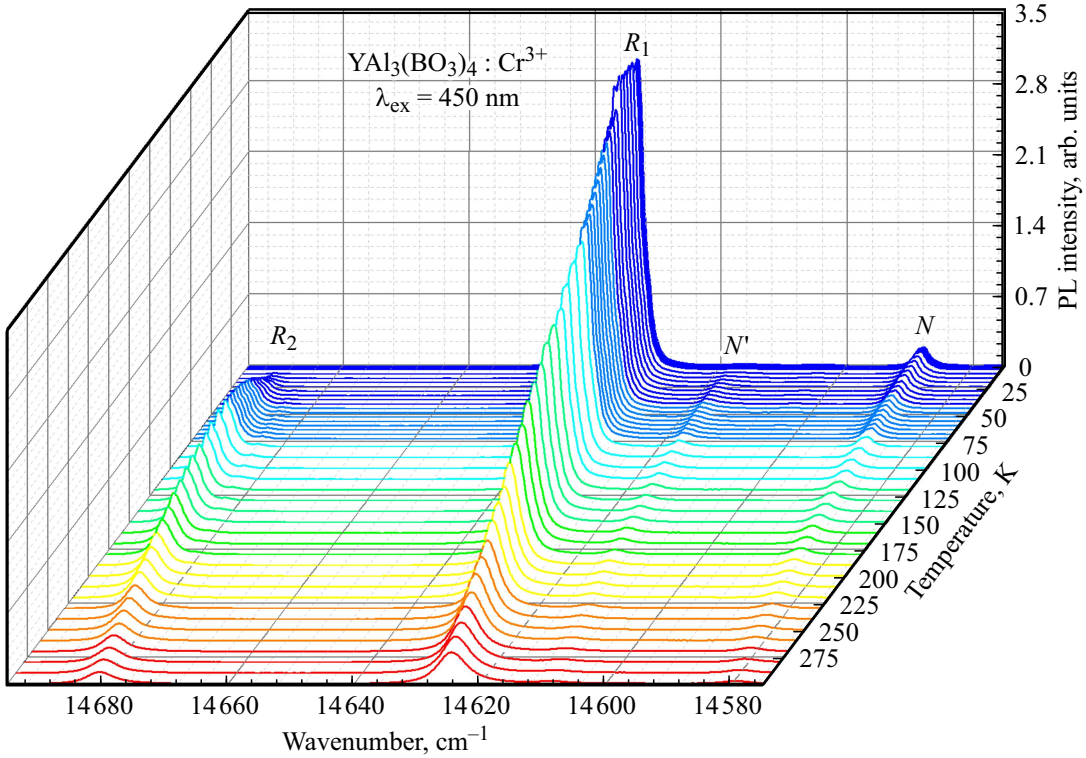

Figure 4. Photoluminescence spectra of a YAB:Cr crystal within the 14550–14700 cm^{-1} frequency range at temperatures of 4–300 K (the wavenumber scale has been modified compared to Figs. 2 and 3: larger values are on the left).

Characteristics of luminescent thermometers based on $YAl_3(BO_3)_4$:Cr^{3+}

Optical parameter	λ, nm	ΔE, cm^{-1}	T_m, K	$S_r(T_m)$, % K^{-1}
$LIR\,[R_2/R_1]$	680–684	56	40.3	5
$LIR[N'/N]$	684–686	30	21.6	9.2
$\Delta\nu(R_1)$	683–684	–	300	2

and N. The experimental curve also follows closely the Boltzmann distribution for the $\Delta E = 30\,cm^{-1}$ interval. It may thus be concluded that lines N and N' belong to the same Cr^{3+} center. Figure 7, *b* presents the temperature dependences of the absolute and relative sensitivities. The maximum absolute sensitivity is achieved at $T_m = 21.6$ K, while the relative sensitivity at this temperature is $S_r(T_m)$ 9.2% K^{-1}.

A summary of all data and the examined characteristics of potential YAB:Cr-based thermometers is given in the table.

Conclusion

A YAB:Cr crystal was examined as a material for luminescent thermometry in the low-temperature region. The measurement of parameters of R lines of Cr^{3+} ions (the $^2E \rightarrow {}^4A_2$ transition) was proposed as a means for temperature recording. YAB:Cr luminescence lines in the region of R lines were identified. The additional recorded N and N' lines were attributed to the $^2E \rightarrow {}^4A_2$ transitions in the Cr^{3+} center at a site distorted by a certain proximate defect. Temperature dependences $LIR(T)$ of ratios of integral intensities of lines R_2 and R_1 and lines N' and N follow Boltzmann distribution $LIR(T) = Ce^{(-\Delta E/kT)}$ closely for $\Delta E = 56\,cm^{-1}$ and $\Delta E = 30\,cm^{-1}$, respectively. Ratiometric luminescent cryothermometers with absolute sensitivity maxima at temperatures of 40.3 and 21.6 K, respectively, may be constructed on the basis of measurement of these ratios. The relative sensitivities at these temperatures are 5 and 9.2% K^{-1}, respectively. Measurement of the width of the most intense spectral component (line R_1) may serve as a means to record temperatures within the range above 100 K.

Funding

This study was supported financially by the Russian Science Foundation (grant No. 19-72-10132P). M.N. Popova acknowledges support from the Ministry of Science and Higher Education of the Russian Federation (project FFUU-2022-0003 under the state assignment of the Institute of Spectroscopy, Russian Academy of Sciences).

Conflict of interest

The authors declare that they have no conflict of interest.

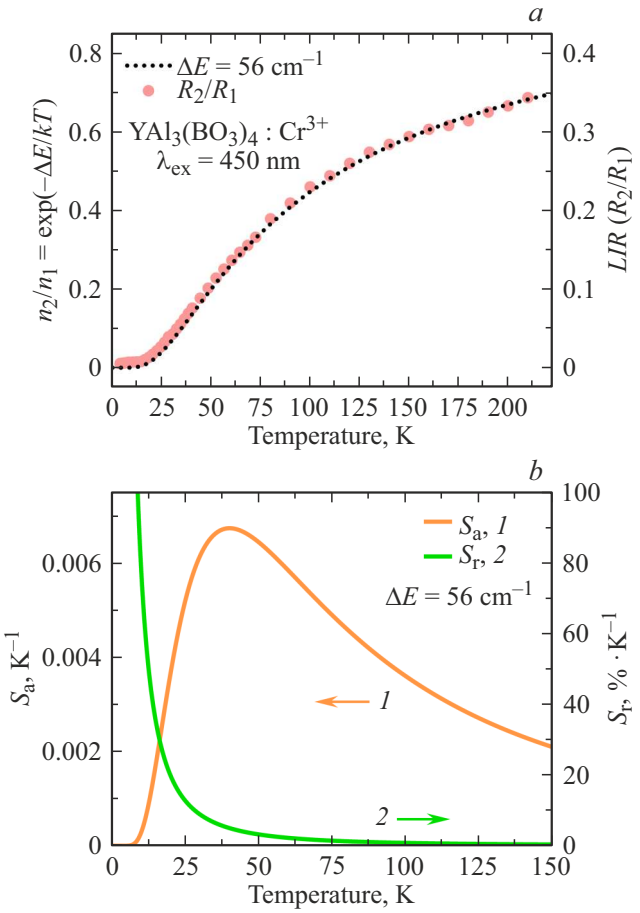

Figure 5. Ratio of intensities of luminescence lines R_2 and R_1. The experimental data are represented by red dots. The black dotted curve is the Boltzmann distribution for $\Delta E = 56\,\text{cm}^{-1}$ (*a*). Absolute sensitivity S_a (orange curve *1*) and relative sensitivity S_r (green curve *2*) for $\Delta E = 56\,\text{cm}^{-1}$ (*b*).

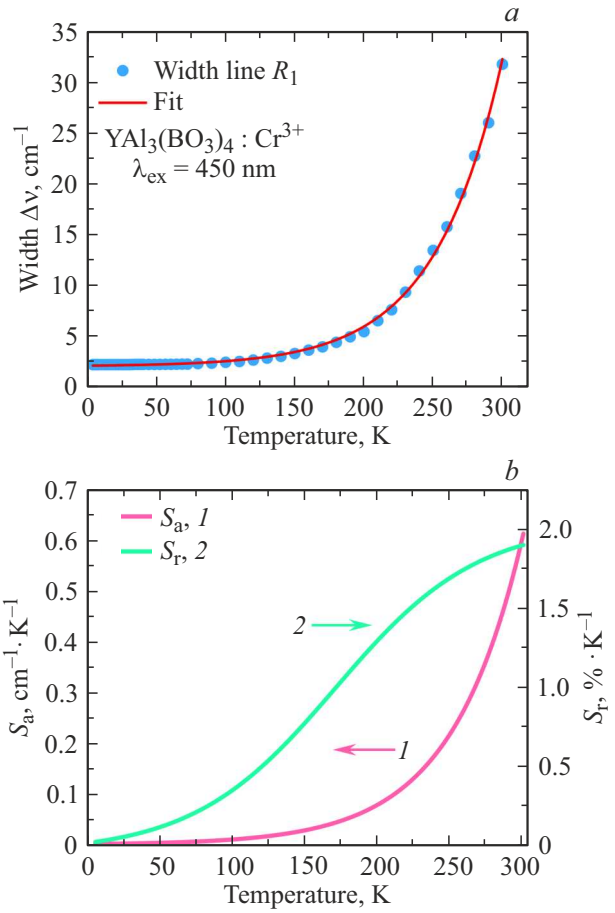

Figure 6. Temperature dependences of half-width $\Delta\nu$ of luminescence line R_1 ($14633\,\text{cm}^{-1}$) (*a*) and absolute S_a (pink curve *1*) and relative S_r (green curve *2*) sensitivities in measurement of $\Delta\nu(R_1)$ (*b*).

References

[1] K. Elzbieciak-Piecka, L. Marciniak. Sci. Rep., **12**, 16364 (2022). DOI:10.1038/s41598-022-20821-4

[2] M. Back, J. Ueda, M.G. Brik, S. Tanabe. ACS Appl. Mater. Interfaces, **12**, 38325 (2020). DOI: 10.1021/acsami.0c08965

[3] M. Back, J. Ueda, M.G. Brik, T. Lesniewski, M. Grinberg, S. Tanabe. ACS Appl. Mater. Interfaces, **10**, 41512 (2018). DOI: 10.1021/acsami.8b15607

[4] M. Back, E. Trave, J. Ueda, S. Tanabe. Chem. Mater., **28**, 8347 (2016). DOI: 10.1021/acs.chemmater.6b03625

[5] A. Mondal, J. Manam. Ceram. Int., **46**, 23972 (2020). DOI: 10.1016/j.ceramint.2020.06.174

[6] M. Back, J. Ueda, H. Nambu, M. Fujita, A. Yamamoto, H. Yoshida, H. Tanaka, M.G. Brik, S. Tanabe. Adv. Opt. Mater., **9**, 2100033 (2021). DOI: 10.1002/adom.202100033

[7] X. Zhang, X. Chen, C. Zhou, J. Fan, W. Zhou, J. Luo, L. Liu, Q. Pang, P. Chen, L. Zhou. Ceram. Int., **48**, 19484 (2022). DOI: 10.1016/j.ceramint.2022.03.252

[8] J. Ueda, M. Back, M.G. Brik, Y. Zhuang, M. Grinberg, S. Tanabe. Opt. Mater., **85**, 510 (2018). DOI: 10.1016/j.optmat.2018.09.013

[9] D. Chen, S. Liu, Z. Wan, Z. Ji. J. Phys. Chem. C, **120**, 21858 (2016). DOI: 10.1021/acs.jpcc.6b08271

[10] Y. Zhu, C. Li, D. Deng, H. Yu, H. Li, L. Wang, C. Shen, X. Jing, S. Xu. J. Lumin., **237**, 118142 (2021). DOI: 10.1016/j.jlumin.2021.118142

[11] L. Marciniak, A. Bednarkiewicz. Sens. Actuators B Chem., **243**, 388 (2017). DOI: 10.1016/j.snb.2016.12.006

[12] A. Ćirić, S. Stojadinović, Z. Ristić, Ž. Antić, M.D. Dramićanin. Sens. Actuators Phys., **331**, 112987 (2021). DOI: 10.1016/j.sna.2021.112987

[13] V. Mykhaylyk, H. Kraus, Y. Zhydachevskyy, V. Tsiumra, A. Luchechko, A. Wagner, A. Suchocki. Sensors, **20**, 5259 (2020). DOI: 10.3390/s20185259

[14] B. Zhu, N. Li, S. Ren, Y. Liu, D. Zhang, Q. Wang, Q. Shi, Q. Wang, S. Li, B. Zhang, W. Wang, C. Liu. Spectrochim. Acta. A: Mol. Biomol. Spectrosc., **264**, 120321 (2022). DOI: 10.1016/j.saa.2021.120321

[15] M. Back, J. Ueda, J. Xu, K. Asami, M. G. Brik, S. Tanabe. Adv. Opt. Mater., **8**, 2000124 (2020). DOI: 10.1002/adom.202000124

[16] M. Suta, A. Meijerink. Adv. Theory Simul., **3**, 2000176 (2020). DOI: 10.1002/adts.202000176

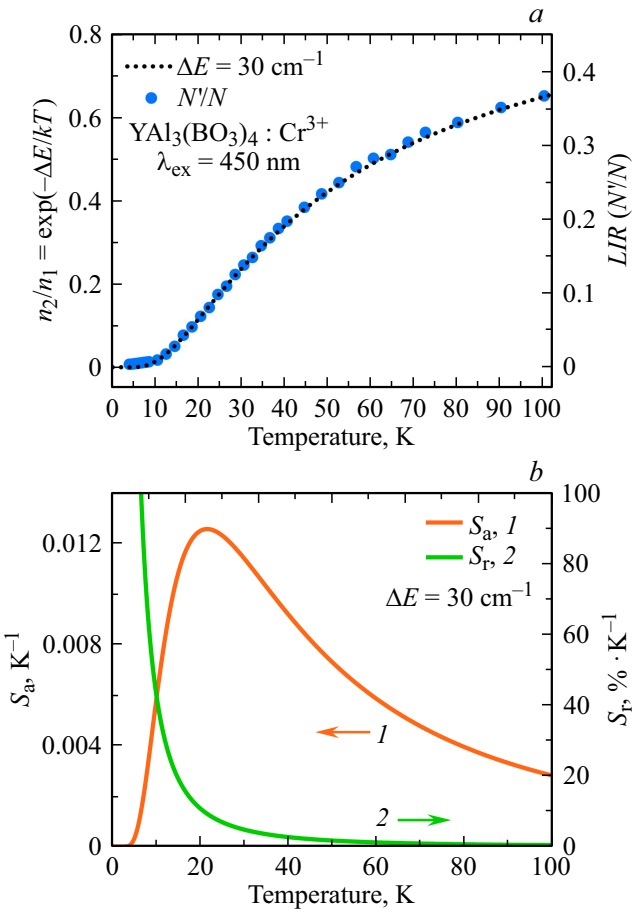

Figure 7. Ratio of intensities of luminescence lines N' and N. The experimental data are represented by blue dots. The black dotted curve is the Boltzmann distribution for $\Delta E = 30\,\mathrm{cm}^{-1}$ (*a*). Absolute sensitivity S_a (orange curve *1*) and relative sensitivity S_r (green curve *2*) at interval $\Delta E = 30\,\mathrm{cm}^{-1}$ (*b*).

[17] N.I. Leonyuk, L.I. Leonyuk. Prog. Cryst. Growth Charact. Mater., **31**, 179 (1995). DOI: 10.1016/0960-8974(96)83730-2
[18] R.D. Shannon. Acta Crystallogr. Sect. A, **32**, 751 (1976). DOI: 10.1107/S0567739476001551
[19] J.-P.R. Wells, M. Yamaga, T.P.J. Han, M. Honda. J. Phys. Condens. Matter., **15**, 539 (2003). DOI: 10.1088/0953-8984/15/3/318
[20] G. Wang, H.G. Gallagher, T.P.J. Han, B. Henderson. J. Cryst. Growth, **153**, 169 (1995). DOI: 10.1016/0022-0248(95)00157-3
[21] G. Wang, H.G. Gallagher, T.P.J. Han, B. Henderson. Radiat. Eff. Defects Solids, **136**, 43 (1995). DOI: 10.1080/10420159508218789
[22] G. Dominiak-Dzik, W. Ryba-Romanowski, M. Grinberg, E. Beregi, L. Kovacs. J. Phys. Condens. Matter., **14**, 5229 (2002). DOI: 10.1088/0953-8984/14/20/318
[23] A. Molchanova, K. Boldyrev, N. Kuzmin, A. Veligzhanin, K. Khaydukov, E. Khaydukov, O. Kondratev, I. Gudim, E. Mikliaeva, M. Popova. Materials, **16**, 537 (2023). DOI: 10.3390/ma16020537
[24] G.F. Imbusch. Phys. Rev., **153**, 326 (1967). DOI: 10.1103/PhysRev.153.326
[25] S.P. Jamison, G.F. Imbusch. J. Lumin., **75**, 143 (1997). DOI: 10.1016/S0022-2313(97)00117-8
[26] B. Malysa, A. Meijerink, T. Jüstel. J. Lumin., **171**, 246 (2016). DOI: 10.1016/j.jlumin.2015.10.042
[27] W. Mikenda, A. Preisinger. J. Lumin., **26**, 53 (1981). DOI: 10.1016/0022-2313(81)90169-1
[28] P. Kisliuk, W.F. Krupke. J. Appl. Phys., **36**, 1025 (1965). DOI: 10.1063/1.1714084

Translated by D.Safin